

## Superselective Targeting Using Multivalent Polymers

Galina V. Dubacheva,<sup>\*,†</sup> Tine Curk,<sup>§</sup> Bortolo M. Moggetti,<sup>§,‡</sup> Rachel Auzély-Velty,<sup>⊥</sup> Daan Frenkel,<sup>§</sup> and Ralf P. Richter<sup>\*,†,||,∇,#</sup>

<sup>†</sup>Biosurfaces Unit, CIC biomaGUNE, Paseo Miramon 182, 20009 Donostia-San Sebastian, Spain

<sup>§</sup>Department of Chemistry, University of Cambridge, Cambridge CB2 1EW, United Kingdom

<sup>‡</sup>Center for Nonlinear Phenomena and Complex Systems, Université Libre de Bruxelles, Campus Plaine, B-1050 Brussels, Belgium

<sup>⊥</sup>Centre de Recherches sur les Macromolécules Végétales, CNRS, and <sup>||</sup>Département de Chimie Moléculaire, Université Joseph Fourier, BP 53, 38041 Grenoble Cedex 9, France

<sup>∇</sup>Max-Planck-Institute for Intelligent Systems, Heisenbergstrasse 3, 70569 Stuttgart, Germany

<sup>#</sup>Department of Biochemistry and Molecular Biology, University of the Basque Country, Barrio Sarriena s/n, 48940 Leioa, Spain

### Supporting Information

**ABSTRACT:** Despite their importance for material and life sciences, multivalent interactions between polymers and surfaces remain poorly understood. Combining recent achievements of synthetic chemistry and surface characterization, we have developed a well-defined and highly specific model system based on host/guest interactions. We use this model to study the binding of hyaluronic acid functionalized with host molecules to tunable surfaces displaying different densities of guest molecules. Remarkably, we find that the surface density of bound polymer increases faster than linearly with the surface density of binding sites. Based on predictions from a simple analytical model, we propose that this superselective behavior arises from a combination of enthalpic and entropic effects upon binding of nanoobjects to surfaces, accentuated by the ability of polymer chains to interpenetrate.

Multivalent interactions take place when multiple ligands of one entity bind to multiple receptors of another one.<sup>1</sup> For linear polymers, their multivalent self-assembly at functional interfaces is an important type of interactions in material, biomedical and life sciences.<sup>1,2</sup> Examples relevant to biological systems include multivalent binding of hyaluronic acid (HA) to cell surfaces.<sup>3</sup> The supramolecular organization of the HA-rich pericellular matrix has been associated with a number of biological processes such as inflammation<sup>4</sup> and tumor development.<sup>5</sup> It is therefore a subject of intensive studies.<sup>6</sup> Multivalent polymers have also been exploited for the design of stimuli-responsive films,<sup>7</sup> therapeutic agents,<sup>8</sup> and gene delivery systems.<sup>8b</sup>

Even though multivalent interactions between polymers and surfaces attract growing interest in material and life sciences, they are still poorly understood, and assaying them remains challenging.<sup>2</sup> Only few experimental model systems relevant to such interfaces have been reported so far.<sup>6a,9</sup> It is generally accepted that multivalency confers strong and irreversible binding, provided that the polymer molecules are long enough. However, further investigation of factors regulating multivalent polymer binding is hindered by (i) insufficient specificity (e.g.,

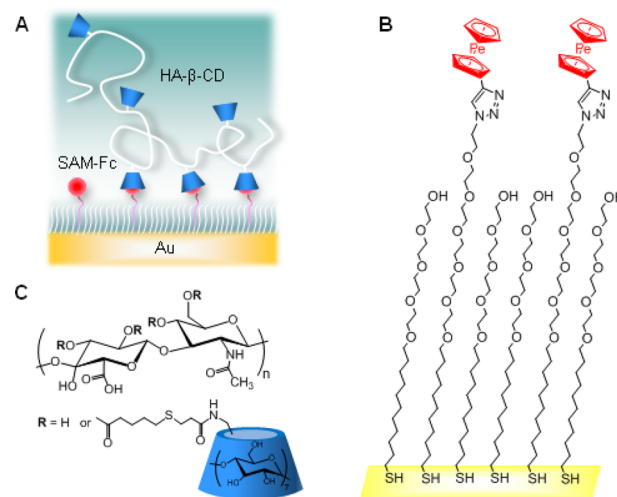


**Figure 1.** Host/guest model system. (A) Schematic representation of HA-β-CD multivalent binding to SAM-Fc. (B) Chemical structure of SAM-Fc. (C) Chemical structure of HA-β-CD.

polymer/polymer interactions<sup>9</sup>), (ii) poor experimental control (e.g., over binding strength between the individual ligands and receptors, or over polymer valency<sup>6a</sup>), and (iii) limited tunability (e.g., of surface density of binding sites<sup>9</sup>).

One of the important aspects of multivalency concerns superselectivity, which implies that the surface density of bound nanoobjects increases faster than linearly with the density of surface binding sites.<sup>10</sup> Such strong dependence on surface coverage allows specific targeting of surfaces displaying binding sites above a threshold surface concentration, while leaving surfaces with lower coverages unaffected. The design of such highly selective nanotherapeutics is one of the key challenges in biomedical sciences.<sup>8b,11</sup> Superselectivity was first theoretically described for multivalent ligand-coated nanoparticles at receptor-functionalized surfaces.<sup>10</sup> Here, we provide evidence for superselectivity in the multivalent binding of polymers to

Received: October 31, 2013

Published: January 9, 2014

surfaces. The ability of flexible polymer chains to deform and interpenetrate implies a rather different binding mechanism compared to nanoparticles. To study the multivalent interaction between polymers and surfaces, we have developed a well-defined and highly specific model system based on host/guest interactions (Figure 1A). Using this experimental platform in combination with a simple analytical model, we demonstrate that multivalent polymers discriminate sharply between surfaces displaying low and high densities of binding sites, thus allowing for superselective targeting.

In this work, we investigated multivalent interactions between self-assembled monolayers (SAMs) functionalized with the guest ferrocene (SAM-Fc, Figure 1B) and HA modified with the host  $\beta$ -cyclodextrin (HA- $\beta$ -CD, Figure 1C). This particular system was chosen because our preliminary tests with SAMs modified with  $\beta$ -CD and HA functionalized with guest groups revealed that HA-guest binds nonspecifically to SAM surfaces. In addition, polymers modified with guest groups may undergo hydrophobic guest/guest interactions within or between polymer chains.<sup>9</sup> To circumvent these undesired polymer/surface and polymer/polymer interactions, we designed a model system where receptors (hosts) are grafted to HA, while ligands (guests) are attached to the surface. We chose HA as a model polymer because of its importance in biological systems and its numerous biomedical applications.<sup>12</sup>  $\beta$ -CD host/guest chemistry is well suited for the experimental modeling of multivalent interactions. First,  $\beta$ -CD complexes are water-soluble at physiological conditions and have a wide affinity range ( $K_d = 10 \mu\text{M}$ – $10 \text{ mM}$ ).<sup>13</sup> Therefore, they can be used to mimic biological interactions like the one between cell surface receptors and HA ( $K_d = 10$ – $100 \mu\text{M}$ ).<sup>6a</sup> In addition, efficient and tunable synthetic strategies exist to graft  $\beta$ -CD and guest molecules to polymers and surfaces.<sup>7,14</sup>

To functionalize HA with  $\beta$ -CD, we first performed the esterification of HA hydroxyl groups using pentenoic anhydride followed by the reaction with a  $\beta$ -CD thiol derivative (see Supporting Information for the details of HA- $\beta$ -CD synthesis). This thiol/ene coupling method was recently introduced for the efficient, mild, and tunable functionalization of polysaccharides.<sup>14</sup> The weight-averaged molecular weight of HA ( $M_{\text{HA}}$ ) used in this study was 357 kg/mol. The degree of substitution, DS = 3% (i.e., the fraction of  $\beta$ -CD-functionalized disaccharides), was determined by integrating the NMR signals arising from the HA and  $\beta$ -CD protons (Figure S1). From the  $M_{\text{HA}}$  and the DS, the average molecular weight of the modified polymer ( $M_{\text{HA-}\beta\text{-CD}}$ ), the average distance between  $\beta$ -CDs along the contour of the polymer chain ( $l_{\beta\text{-CD}}$ ), and the average number of  $\beta$ -CDs per polymer chain were calculated to be 405 kg/mol, 33 nm, and 27, respectively.

To produce SAM-Fc, we first formed mixed SAMs on gold surfaces using HS-(CH<sub>2</sub>)<sub>11</sub>-EG<sub>6</sub>-N<sub>3</sub> and HS-(CH<sub>2</sub>)<sub>11</sub>-EG<sub>4</sub>-OH (EG = ethylene glycol). The EG-terminated thiols are known to effectively suppress undesired nonspecific interactions.<sup>7,15</sup> The SAMs were subsequently functionalized with ferrocene using an azide/alkyne click reaction (see Supporting Information for the details of SAM-Fc formation). Recently introduced, this two-step procedure gives stable and homogeneous monolayers with a tunable surface density of functional groups.<sup>7</sup> Ferrocene was chosen as a guest because its well-defined redox properties can be used to quantify its surface coverage ( $\Gamma_{\text{Fc}}$ ). More specifically,  $\Gamma_{\text{Fc}}$  was determined from the anodic charge associated with the conversion of Fc to Fc<sup>+</sup> (Figure S2). By systematically varying the fraction of HS-(CH<sub>2</sub>)<sub>11</sub>-EG<sub>6</sub>-N<sub>3</sub> during SAM formation, we

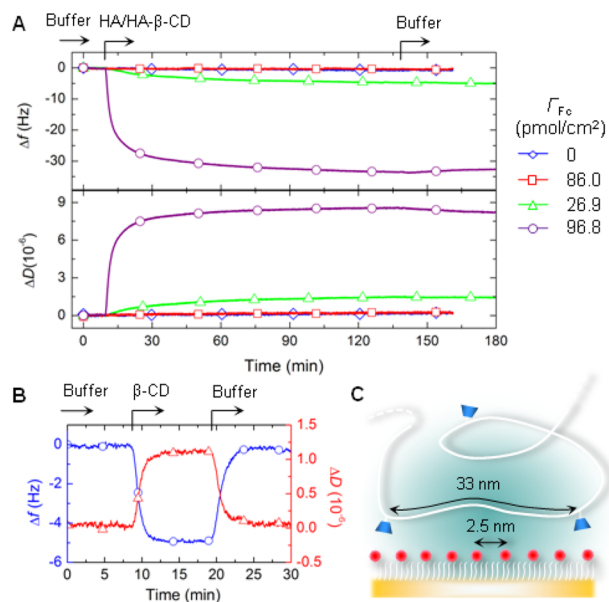


**Figure 2.** Interactions between HA- $\beta$ -CD and SAM-Fc. (A) QCM-D response:  $\Delta f$  and  $\Delta D$  obtained for the multivalent binding of HA- $\beta$ -CD to SAM-Fc (purple circles, green triangles), HA<sub>p</sub> to SAM-Fc (red squares), and HA- $\beta$ -CD to SAM (blue lozenges). (B) QCM-D response:  $\Delta f$  (blue circles) and  $\Delta D$  (red triangles) obtained for the monovalent binding of  $\beta$ -CD to SAM-Fc ( $\Gamma_{\text{Fc}} = 86.0 \text{ pmol/cm}^2$ ). Conditions:  $T = 23 \text{ }^\circ\text{C}$ ;  $c_{\text{HA/HA-}\beta\text{-CD}} = 50 \mu\text{g/mL}$ ;  $c_{\beta\text{-CD}} = 5 \text{ mM}$ . (C) Illustration (not to scale) of average distances between guests on the SAM-Fc surface ( $\Gamma_{\text{Fc}} = 96.8 \text{ pmol/cm}^2$ ) and hosts along the HA- $\beta$ -CD chain.

tuned  $\Gamma_{\text{Fc}}$  and hence the average lateral distance between ferrocene molecules ( $l_{\text{Fc}}$ ; assuming ferrocene molecules to be packed in a square lattice) from 1.6 to 328.5 pmol/cm<sup>2</sup> and from 10 to 0.7 nm, respectively.

To confirm that nonspecific interactions do not interfere with host/guest binding, several test measurements were performed using quartz crystal microbalance with dissipation monitoring (QCM-D). Figure 2A shows the QCM-D response, i.e., shifts in frequency ( $\Delta f$ ) and dissipation ( $\Delta D$ ), recorded upon exposure of (i) HA- $\beta$ -CD to SAM-Fc, (ii) HA<sub>p</sub> to SAM-Fc, and (iii) HA- $\beta$ -CD to SAM (HA<sub>p</sub> = HA modified with pentenoate, the precursor for the synthesis of HA- $\beta$ -CD). As desired, no shifts were observed for scenarios (ii) and (iii), whereas a pronounced negative frequency shift was detected in case (i), indicating binding. The concomitant strong increase in dissipation indicates that HA- $\beta$ -CD forms a soft film, with the locally attached HA chains presumably having many tails and loops that dangle into the solution. The high stability of the HA- $\beta$ -CD film upon buffer rinsing is in agreement with previous studies<sup>6a,9b</sup> and is indicative of the multivalent nature of host/guest interactions. For comparison, monovalently bound  $\beta$ -CD molecules undergo fast and complete desorption during rinsing (Figure 2B). The absence of nonspecific interactions together with the stable polymer attachment provide evidence that HA- $\beta$ -CD binding to SAM-Fc occurs entirely through multivalent host/guest interactions.

Figure 2A also shows that multivalent attachment of HA- $\beta$ -CD to SAM-Fc strongly depends on the ferrocene surface density: a 6-fold decrease in  $f$  and  $D$  shifts occurs when  $\Gamma_{\text{Fc}}$  is reduced from 96.8 to 26.9 pmol/cm<sup>2</sup>. Interestingly, such a strong effect occurs even though the average distances between guest molecules on both surfaces ( $l_{\text{Fc}} = 1.3$  and 2.5 nm, respectively) remain far

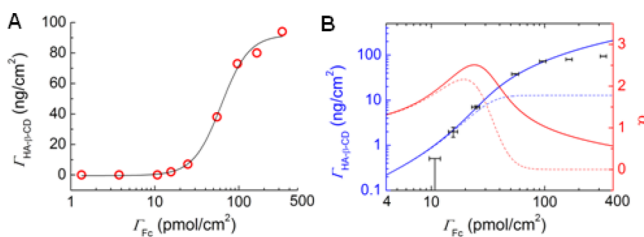


**Figure 3.** Characterization of HA- $\beta$ -CD selectivity to  $\Gamma_{\text{Fc}}$ . (A)  $\Gamma_{\text{HA-}\beta\text{-CD}}$  determined by SE as a function of  $\Gamma_{\text{Fc}}$ . Conditions:  $T = 23^\circ\text{C}$ ,  $c_{\text{HA-}\beta\text{-CD}} = 50\ \mu\text{g/mL}$ . The solid black line is a guide for the eyes. (B) Experimental data from (A) replotted in the form of error bars (black) in log-log scale. For the lowest  $\Gamma_{\text{HA-}\beta\text{-CD}}$ , only an upper limit is given, corresponding to the sensitivity of our SE setup ( $0.5\ \text{ng/cm}^2$ ). The solid and dashed blue lines are a fit and a prediction, respectively, with the analytical model, as described in the main text. The red lines show the respective dependencies of  $\alpha$  on  $\Gamma_{\text{Fc}}$ .

below the average distance between  $\beta$ -CDs along the polymer chains ( $l_{\beta\text{-CD}} = 33\ \text{nm}$ , Figure 2C). Considering that the binding strength of individual  $\beta$ -CD/ferrocene interactions ( $K_{\text{d}} = 250\ \mu\text{M}$ )<sup>16</sup> should be independent of the Fc surface density, this illustrates that the strong nonlinear dependence of polymer binding on surface valency cannot be understood as a purely enthalpic effect (i.e., determined by the number of host/guest inclusion complexes per polymer). Instead, we propose that entropic effects, in the form of costs associated with the reduced conformational freedom of the polymer upon surface binding and with gains in combinatorial entropy with increasing surface density of binding sites,<sup>17</sup> play an important role in setting the HA- $\beta$ -CD selectivity to surfaces displaying different  $\Gamma_{\text{Fc}}$ .

To understand how sharply multivalent polymers discriminate between surfaces with low and high valency, we studied HA- $\beta$ -CD binding to several SAM-Fc samples, where  $\Gamma_{\text{Fc}}$  was changed from 1.6 to 328.5 pmol/cm<sup>2</sup> (i.e.,  $l_{\text{Fc}}$  from 10 to 0.7 nm). This corresponds to between 0.4 and 73% of the maximal attainable Fc coverage (450 pmol/cm<sup>2</sup> considering a close-packed monolayer of ferrocene, with Fc molecules idealized as spheres of 0.66 nm diameter<sup>18</sup>). For each sample, we first performed electrochemical measurements to determine  $\Gamma_{\text{Fc}}$  (Figure S2). Then, upon exposure to HA- $\beta$ -CD, we used spectroscopic ellipsometry (SE) to determine the surface density of the bound polymer  $\Gamma_{\text{HA-}\beta\text{-CD}}$  (Figure S3). The results are shown in Figure 3A.

To evaluate the specificity of binding toward ligand coverage, the selectivity parameter  $\alpha$  has been introduced,<sup>10</sup> reflecting how fast the relative increment of bound nanoobjects (here  $d\Gamma_{\text{HA-}\beta\text{-CD}}/\Gamma_{\text{HA-}\beta\text{-CD}} = d \ln \Gamma_{\text{HA-}\beta\text{-CD}}$ ) changes with the relative increment of ligand surface density (here  $d\Gamma_{\text{Fc}}/\Gamma_{\text{Fc}} = d \ln \Gamma_{\text{Fc}}$ ), i.e.,  $\alpha \equiv d \ln \Gamma_{\text{HA-}\beta\text{-CD}}/d \ln \Gamma_{\text{Fc}}$ . For nonselective binding,  $\alpha$  never exceeds 1, whereas for systems exhibiting superselectivity,  $\alpha$  can reach locally values  $>1$ . This implies that a slight variation in the receptor surface density causes a rapid (nonlinear) change in the surface density of nanoobjects of  $\Gamma_{\text{HA-}\beta\text{-CD}} = \Gamma_{\text{Fc}}^\alpha$ . As shown in Figure 3B,  $\Gamma_{\text{HA-}\beta\text{-CD}}$  increases nonlinearly with the surface density of ferrocene until  $\Gamma_{\text{Fc}} = 100\ \text{pmol/cm}^2$ , corresponding to  $\sim 30\%$  of the maximal coverage. Taking into account experimental uncertainties, we determined that  $\alpha$  can reach values of at least 2.6. This is direct experimental evidence that our multivalent polymers exhibit a degree of superselectivity, which is at least as strong as was predicted theoretically for nanoparticles.<sup>10</sup> We note that our current system is not yet optimized in terms of polymer valency, polymer concentration, and binding strength of

individual host/guest interactions. These parameters were predicted to influence selectivity in multivalent systems.<sup>10</sup> One can therefore expect that multivalent polymers can exhibit even higher  $\alpha$  values once binding conditions are optimized.

To rationalize the superselective behavior in the multivalent binding of polymers to surfaces, we developed a simple analytical model, inspired by the approach previously developed for multivalent particles.<sup>10</sup> In contrast to particles, polymer chains can interpenetrate. We therefore developed a generalized version of the model where, in principle, multiple nanoobjects can adsorb to the same location on a surface. Details are described in the Supporting Information (including Figures S4 and S5), and only the main features are presented here.

We consider a simple coarse-grained model, where the surface is divided into cells of size  $a^2$ , where  $a$  is about the size of the nanoobject (in our case  $a^3 = (4/3)\pi R_{\text{g}}^3$ , where  $R_{\text{g}} \approx 45\ \text{nm}$  is the polymer's radius of gyration; see Supporting Information for details). On average, each cell contains  $n_{\text{L}}$  ligands (here,  $n_{\text{L}} = \Gamma_{\text{Fc}}N_{\text{A}}a^2$ , where  $N_{\text{A}}$  is Avogadro's number), and each polymer chain carries  $n_{\text{R}}$  receptors (here,  $n_{\text{R}} = 27$ ) that can bind to the ligands. We assume that each polymer chain has access to only a single cell at a time, but within a cell, all of the receptors are within reach of all the ligands. The volume available to a polymer, while bound to a cell, is  $\sim a^3$ . For this model we can analytically calculate the average number of bound polymers per cell as

$$\theta(n_{\text{L}}) = \sum_i iz^i q_i / (1 + \sum_i z^i q_i) \quad (1)$$

where the sum goes over all possible numbers  $i$  of polymers in a cell. In dilute solutions, the activity  $z$  of polymers is given by  $z \approx cN_{\text{A}}a^3/M_{\text{w}}$ , where  $c$  is the polymer concentration (here  $50\ \mu\text{g/mL}$ ).  $q_i$  is the bound state partition function which, in a given cell, counts all possible bonding arrangements between  $i$  polymers and  $n_{\text{L}}$  surface ligands. For the range of parameters studied here, the number of ligands per cell is always much larger than the number of receptors, and in this case we can use a simplified form for  $q_i$

$$q_i = \frac{1}{i!} [(1 + n_{\text{L}} e^{-F/k_{\text{B}}T})^{n_{\text{R}}} - 1]^i e^{-U_i/k_{\text{B}}T} \quad (2)$$

where  $T$  is the absolute temperature and  $k_{\text{B}}$  the Boltzmann constant.  $F$  is the ligand/receptor binding free energy, which determines the probability that a particular ligand is bound when a polymer is in the cell. We can estimate  $F$  from the dissociation constant  $K_{\text{d}}$  of individual ligand/receptor interactions through  $F = \ln(K_{\text{d}}a^3N_{\text{A}})k_{\text{B}}T + U_{\text{poly}}$ , where  $U_{\text{poly}}$  represents added entropic effects associated with ligand/receptor bond formation, once the nanoobject is present at the surface.  $U_{\text{poly}}$  is expected to be on the order of a few  $k_{\text{B}}T$ ,<sup>17</sup> and is treated here as a fitting parameter.  $U_i$  specifies the free energy penalty for the interpenetration of  $i$  polymer coils. In a simple scaling approximation,  $U_i = A_{\text{dG}}i^{9/4}$ , where  $A_{\text{dG}}$  is a prefactor that we expect to be of order  $k_{\text{B}}T$ , and the number of polymers per cell  $i$  is proportional to the packing fraction. At high ligand coverages, where  $i$  becomes large, the scaling approximation is likely to be an underestimate, because in the presence of many ligand/receptor bonds per polymer, the film of adsorbed polymers is expected to exhibit a steep density profile,<sup>19</sup> and the effective packing fraction close to the surface therefore becomes larger than  $i$ .

The blue solid line in Figure 3B, representing  $\Gamma_{\text{HA-}\beta\text{-CD}} = \theta M_{\text{HA-}\beta\text{-CD}}/N_{\text{A}}a^2$ , is the result of a fit to our experimental data with the analytical model using two adjustable parameters:  $A_{\text{dG}}$  and  $U_{\text{poly}}$ . As outlined above, the model is not expected to capture



all the details of our experimental system. In particular, the model neglects correlations between the spatial positions of polymer-bound receptors. It also assumes the polymers to adsorb into discrete cells of fixed size, whereas adsorption can occur on a continuous surface in reality, and the surface area occupied by a polymer chain may depend somewhat on the state of adsorption. Given the simplicity of the model and the small number of fitting parameters, the agreement between the experiments and analytical results is remarkable. In particular, the model quantitatively reproduces the experimentally observed polymer densities in the range of ligand surface densities that exhibit the largest  $\alpha$ . Moreover, the resulting values of  $A_{dG} = 0.35k_B T$  and  $U_{poly} = 4.55k_B T$  are of the expected order of magnitude. As outlined earlier, the overestimation of surface coverages by the theory at the largest ligand surface densities is not unexpected.

The agreement between the experimental and analytical results implies that polymer superselectivity is indeed a consequence of multivalency. The multivalent effects (i.e., combinatorial entropic gain and polymer valency<sup>10</sup>) are hidden in the expression for the bound state partition function  $q_b$ , which depends nonlinearly on the number of ligands  $n_L$  (eq 2). If we were to use monovalent polymers ( $n_R = 1$ ) and allow for at most a single polymer per cell ( $i_{max} = 1$ ), then our model (eq 1) would recover the well-known Langmuir adsorption isotherm. The developed theoretical model also suggests that superselective behavior of linear polymers is influenced by their ability to interpenetrate ( $i > 1$ ). For comparison, results are also shown for a system in which the maximal number of nanoobjects per cell was limited to one ( $i_{max} = 1$ ), with all other parameters kept identical (dashed curves in Figure 3B). This scenario corresponds to the binding of multivalent particles as previously presented.<sup>10</sup> In this case, binding saturates at lower ligand densities than for polymers. Interestingly, the range of ligand densities in which binding is superselective ( $\alpha > 1$ ) broadens and the quality of the selectivity, i.e., the peak in  $\alpha$ , is larger for polymers. This indicates that, owing to their flexible nature and the associated propensity to interpenetrate, polymers can in principle offer superior selectivity compared to other multivalent scaffolds such as particles.

In addition, the developed analytical model predicts that the obtained findings can be extended to biologically relevant conditions. In particular, when the HA valency matches the footprint of HA binding proteins, the position of the peak in  $\alpha$  shifts to lower surface coverages (Figure S5B), comparable to the densities of HA cell surface receptors (e.g., CD44<sup>6a</sup>). Importantly, the quality of superselectivity is essentially unaltered under these conditions (Figure S5B).

In summary, we have developed a well-defined and highly specific model system to study multivalent interactions between polymers and surfaces. Using this experimental platform in combination with analytical modeling, we demonstrated that multivalent polymers can exhibit a pronounced superselective binding behavior. The potential tunability of the developed model (e.g., in terms of binding strength of individual host/guest interactions, polymer valency, polymer linker) shall be explored in future work and should provide additional mechanistic insights into the regulation of superselective binding. It should help to understand the regulation of multivalent interactions in biological systems and provide means for the rational design of polymers for tunable, superselective targeting. This paradigm can be of value for the design of effective polymer-based therapeutic agents and drug delivery systems.

## ■ ASSOCIATED CONTENT

### 📄 Supporting Information

Materials and methods. This material is available free of charge via the Internet at <http://pubs.acs.org>.

## ■ AUTHOR INFORMATION

### Corresponding Author

gdubacheva@cicbiomagune.es; rrichter@cicbiomagune.es

### Notes

The authors declare no competing financial interest.

## ■ ACKNOWLEDGMENTS

This work was supported by the Marie Curie Career Integration Grant “CELLMULTIVINT” (PCIG09-GA-2011-293803) to G.V.D., the European Research Council Starting Grant “JELLY” (306435) to R.P.R., and the Herchel Smith Fund to T.C. L. Yate and J. Calvo (CIC biomaGUNE) are acknowledged for providing metal surface coatings and help with mass spectrometry analysis, respectively. We thank F. J. Martinez-Veracoechea and O. V. Borisov for fruitful discussions.

## ■ REFERENCES

- (1) Mammen, M.; Choi, S.-K.; Whitesides, G. M. *Angew. Chem., Int. Ed.* **1998**, *37*, 2754.
- (2) Fasting, C.; Schalley, C. A.; Weber, M.; Seitz, O.; Hecht, S.; Koks, B.; Dervede, J.; Graf, C.; Knapp, E.-W.; Haag, R. *Angew. Chem., Int. Ed.* **2012**, *51*, 10472.
- (3) Lesley, J.; Hascall, V. C.; Tammi, M.; Hyman, R. J. *Biol. Chem.* **2000**, *275*, 26967.
- (4) Puré, E.; Cuff, C. A. *Trends Mol. Med.* **2001**, *7*, 213.
- (5) Toole, B. P. *Clin. Cancer Res.* **2009**, *15*, 7462.
- (6) (a) Wolny, P. M.; Banerji, S.; Gounou, C.; Brisson, A. R.; Day, A. J.; Jackson, D. G.; Richter, R. P. *J. Biol. Chem.* **2010**, *285*, 30170. (b) Yang, C.; Cao, M.; Liu, H.; He, Y.; Xu, J.; Du, Y.; Liu, Y.; Wang, W.; Cui, L.; Hu, J.; Gao, F. *J. Biol. Chem.* **2012**, *287*, 43094.
- (7) Dubacheva, G. V.; Van Der Heyden, A. I.; Dumy, P.; Kaftan, O.; Auzély-Velty, R.; Coche-Guerente, L.; Labbé, P. *Langmuir* **2010**, *26*, 13976.
- (8) (a) Daniai, M.; Root, M. J.; Klok, H.-A. *Biomacromolecules* **2012**, *13*, 1438. (b) Duncan, R. *Nat. Rev. Cancer* **2006**, *6*, 688.
- (9) (a) Ravoo, B. J.; Jacquier, J.-C.; Wenz, G. *Angew. Chem., Int. Ed.* **2003**, *42*, 2066. (b) Crespo-Biel, O.; Péter, M.; Bruinink, C. M.; Ravoo, B. J.; Reinhoudt, D. N.; Huskens, J. *Chem.—Eur. J.* **2005**, *11*, 2426.
- (10) Martinez-Veracoechea, F. J.; Frenkel, D. *Proc. Natl. Acad. Sci. U.S.A.* **2011**, *108*, 10963.
- (11) Schroeder, A.; Heller, D. A.; Winslow, M. M.; Dahlman, J. E.; Pratt, G. W.; Langer, R.; Jacks, T.; Anderson, D. G. *Nat. Rev. Cancer* **2012**, *12*, 39.
- (12) (a) Burdick, J. A.; Prestwich, G. D. *Adv. Mater.* **2011**, *23*, H41. (b) Fraser, J. R. E.; Laurent, T. C.; Laurent, U. B. G. *J. Intern. Med.* **1997**, *242*, 27. (c) Morra, M. *Biomacromolecules* **2005**, *6*, 1205.
- (13) Rekharsky, M. V.; Inoue, Y. *Chem. Rev.* **1998**, *98*, 1875.
- (14) Mergy, J.; Fournier, A.; Hachet, E.; Auzély-Velty, R. *J. Polym. Sci., Part A: Polym. Chem.* **2012**, *50*, 4019.
- (15) Dubacheva, G. V.; Galibert, M.; Coche-Guerente, L.; Dumy, P.; Boturyn, D.; Labbe, P. *Chem. Commun.* **2011**, *47*, 3565.
- (16) Osella, D.; Carretta, A.; Nervi, C.; Ravera, M.; Gobetto, R. *Organometallics* **2000**, *19*, 2791.
- (17) Martinez-Veracoechea, F. J.; Leunissen, M. E. *Soft Matter* **2013**, *9*, 3213.
- (18) Chidsey, C. E. D.; Bertozzi, C. R.; Putvinski, T. M.; Muijsce, A. M. *J. Am. Chem. Soc.* **1990**, *112*, 4301.
- (19) de Gennes, P.-G. *Scaling concepts in polymer physics*; Cornell University Press: Ithaca, NY, 1979.